# Anomalous heat conduction in polyethylene chains: Theory and molecular dynamics simulations

Asegun Henry and Gang Chen
*Department of Mechanical Engineering, Massachusetts Institute of Technology, 77 Massachusetts Avenue, Cambridge, Massachusetts 02139, USA*

(Received 7 January 2009; revised manuscript received 31 March 2009; published 24 April 2009)

In 1955 Fermi, Pasta, and Ulam showed that a simple model for a nonlinear one-dimensional chain of particles can be nonergodic, which implied infinite thermal conductivity. A more recent investigation of a realistic model for an individual polyethylene chain suggests that this phenomenon can even persist in real polymer chains. The reason for the divergent behavior and its associated mechanism, however, remains unclear. This paper presents a general formulation for normal-mode vibrational contributions to thermal conductivity, which is then used to analyze molecular dynamics simulations of individual polyethylene chains. Our analysis shows that cross correlations for midfrequency longitudinal-acoustic phonons are responsible for the divergent thermal conductivity in our model.

DOI: 10.1103/PhysRevB.79.144305 PACS number(s): 63.22.−m, 63.20.D−, 63.20.kg, 66.70.Hk

## I. INTRODUCTION

Fermi, Pasta, and Ulam's[1] (FPU) "remarkable little discovery" that nonlinear chains of oscillators can be nonergodic led to the discovery of solitons and gave birth to the modern field of computational nonlinear dynamics.[2,3] The FPU problem was originally proposed in order to study the system's rate of thermalization and approach to equilibrium. This was based on an expected evolution toward an equipartition of mode energy, as a result of the mode-mode interactions induced by the nonlinear particle interactions. The surprising recurrence phenomenon that was observed suggested that even an anharmonic chain of oscillators can have infinite thermal conductivity.[2,3]

Since the FPU discovery, the idea of anomalous heat conduction has been more thoroughly investigated,[2,4–15] shedding light on the possibility for engineering thermal superconductors through ballistic heat conduction. Most previous works have investigated fictitious systems,[2,4–14] where the interactions between particles were chosen for better understanding of the circumstances required for infinite conductivity. Although some have conjectured that anomalous heat conduction can occur in carbon nanotubes,[16] less restrictive analysis indicates finite scattering rates and eventual convergence of thermal conductivity with increasing tube length.[17] Our recent simulations of individual polymer chains,[15] on the other hand, have indicated the potential for anomalous heat conduction through the divergence of Green-Kubo integrals.

Our polyethylene chain model differs from previous works[13,14,18] in the sense that we used a more realistic chemical bonding based description of the atomic interactions through the adaptive intermolecular reactive empirical bond order (AIREBO) potential.[15,19,20] In this model, the motion of hydrogen atoms can affect the bonding between neighboring pairs of carbon atoms through many-body angular terms. The explicit treatment of both carbon and hydrogen atoms in this model also leads to a wide spectrum of optical phonon frequencies ranging from ~30–85 THz. Although these optical modes are expected to have small contributions to the conductivity, they can reduce the thermal conductivity by scattering lower frequency acoustic modes.[21] This added complexity was neglected in earlier works, which either studied fictitious molecules or employed united atom models.[2,4–14] The explicit treatment of hydrogen atoms also leads to interesting interactions between different polarizations.[20] The ramifications of these effects, however, have not been studied thoroughly in the literature.

For heat conduction in crystalline materials, it is common to start from the Boltzmann equation to derive an expression for the thermal conductivity.[22] This approach depicts thermal conductivity as proportional to the average time between phonon collisions. From this perspective, a system having infinite thermal conductivity implies that some phonons do not experience phonon-phonon collisions (umklapp scattering[23]) and therefore conduct heat ballistically. In the FPU problem, however, phonon-phonon collisions (mode-mode interactions) do occur from the nonlinear forces between particles. How is it that phonon-phonon collisions can occur, giving rise to a finite nonzero scattering rate, and yet the thermal conductivity is still infinite? Over the years, it has proved quite difficult to explain this phenomenon with Boltzmann equation based arguments. Later, we will discuss how this issue arises out of the Stosszahlansatz assumption of "molecular chaos," which is used to simplify the scattering integral.[24] Here we present an interpretation of anomalous heat conduction based on mode-mode cross correlations. Our interpretation points to a mechanism that is not intuitively captured by the widely used expressions for thermal conductivity based on the Boltzmann equation,[25] which assume that phonon-phonon collisions are chaotic and uncorrelated.[24]

In this paper we present more detailed analysis of the same model[15] for an individual polyethylene chain, which was previously used to demonstrate the potential for divergence (infinite thermal conductivity). We first derive the expressions used to analyze the simulations and then provide our interpretation of their meaning. We then proceed to a description of the model and simulation procedures. We later show correspondence between the simulation results and our correlation based explanation of the divergent Green-Kubo integrals. Our analyses indicate that the longitudinal-acoustic modes are associated with the processes responsible for the divergent thermal conductivity in polyethylene chains.

 

## II. SIMULATION ANALYSIS

We first consider the Green-Kubo expression for thermal conductivity, which is based on linear-response theory,[22,26]

$$\kappa = \frac{V}{k_B T^2} \int_0^\infty \langle Q_z(t) Q_z(t+t') \rangle dt', \tag{1}$$

where $k_B$ is Boltzmann's constant, $T$ is the system temperature, $V$ is the system volume, and $\langle Q_z(t) Q_z(t+t') \rangle$ is the heat flux autocorrelation function. $Q_z$ represents the component of the heat flux vector $\mathbf{Q}$ directed along the polyethylene chain axis, which is the direction of interest. For the AIREBO potential, which was used to model the atomic interactions, Hardy's derivation[27] of the quantum heat flux operator can be employed to determine $Q_z$,

$$Q_z = \frac{1}{V} \sum_i \left[ E_i \cdot \mathbf{v}_i + \sum_j (-\nabla_{\mathbf{r}_i} \Phi_j \cdot \mathbf{v}_i) \cdot \mathbf{r}_{ij} \right] \cdot \hat{\mathbf{z}}, \tag{2}$$

where the sum is over each atom $i$ in the system which has energy $E_i$, velocity $\mathbf{v}_i$, and potential energy $\Phi_i$ while $\mathbf{r}_{ij}$ denotes the displacement between atoms $i$ and $j$.

This equilibrium approach was chosen because it has shown good agreement with experiments[28–34] and has several advantages over nonequilibrium methods. For one, the equilibrium Green-Kubo method naturally incorporates the use of periodic boundary conditions, in the sense that it allows for calculation of the thermal conductivity in the infinite system size limit, where boundary scattering is nonexistent. Nonequilibrium approaches,[16,18] on the other hand, apply heat flux or temperature boundary conditions to certain regions of atoms by local alteration of the atomic vibration dynamics. The regions where these conditions are applied subsequently induce an artificial form of phonon scattering, which functions as a pseudoboundary. As a result, nonequilibrium approaches induce finite-size effects and require that the simulation domain be larger than the phonon mean-free paths for convergence of the results.[16] For mechanically soft low thermal-conductivity materials with short mean-free paths, this approach is both intuitive and computationally efficient. For stiff high thermal-conductivity materials, where the mean-free paths are long, this method can require large simulation domains that are exceedingly computationally expensive. For the case of a single polyethylene chain, which is stiff, the longitudinal-acoustic phonons have group velocities $>16\,000$ m/s.[15,35] Relaxation time estimates for these phonons exceed 10 ps,[15] and therefore suggest that they propagate ballistically in chains with submicron lengths. If nonequilibrium approaches were used to investigate potentially anomalous heat conduction in polyethylene,[18] we would expect boundary scattering to dominate until the chain lengths were at least several microns long. This would require system sizes larger than 20 000 atoms, which are currently too computationally expensive.

The other major benefit of equilibrium simulations is that they do not involve tampering with the natural atomic vibration. This allows us to study phonon-phonon interactions and temperature-dependent anharmonic effects in isolation, without boundary effects. The major drawback to equilibrium approaches, however, is that they require long simulation times for sufficient phase-space sampling. The other drawback to the Green-Kubo method is that the trajectory data for an entire simulation of $N$ atoms only results in a single value/tensor for thermal conductivity, and does not provide detailed information about the phonon transport. Modal analysis,[15,29–31,33] however, can provide much more detail about the $3N$ modes and can be used in tandem with the Green-Kubo method to analyze the atomic trajectories. This approach[15,29,31] involves projecting the atomic trajectory onto the normal-mode shapes via the following spatial Fourier transformation,

$$X(\mathbf{k},p,t) = \sum_j \sqrt{\frac{m_j}{N}} \cdot [\mathbf{r}_j(t) - \mathbf{r}_{j0}] \cdot \mathbf{p}_j(\mathbf{k},p) \cdot \exp(i \cdot \mathbf{k} \cdot \mathbf{r}_{j0}), \tag{3}$$

where the sum is over all atoms in the system, $m_j$ is the mass of atom $j$, $\mathbf{r}_{j0}$ is its equilibrium position while $\mathbf{r}_j(t)$ is its time dependent position. The indices $\mathbf{k}$ and $p$ denote the wave vector and polarization of each mode while $\mathbf{p}$ is the mode eigenvector determined from lattice dynamics methods.[36] The mode displacements, $X$, can then be used to calculate each mode's total energy after each simulation time step,

$$E(\mathbf{k},p,t) = \left( \frac{X(\mathbf{k},p,t) \cdot X^*(\mathbf{k},p,t) \cdot \omega^2}{2} \right) + \left( \frac{\dot{X}(\mathbf{k},p,t) \cdot \dot{X}^*(\mathbf{k},p,t)}{2} \right), \tag{4}$$

where $\omega$ is the mode frequency, $\dot{X}$ is the time derivative of $X$, and $X^*$ is its complex conjugate. The mode energy is proportional to the mode occupation $E(\mathbf{k},p,t) = h\nu[n(t) + \frac{1}{2}]$. The deviation from average energy $\delta E(\mathbf{k},p,t) = E(\mathbf{k},p,t) - \langle E(\mathbf{k},p) \rangle$ is therefore proportional to the deviation from average occupation $\delta E(\mathbf{k},p,t) \propto \delta n(t)$ and can be used to determine the mode's attenuation rate

$$\tau(\mathbf{k},p) = \frac{\int \langle \delta E(\mathbf{k},p,t) \cdot \delta E(\mathbf{k},p,t+t') \rangle dt'}{\langle \delta E(\mathbf{k},p,t)^2 \rangle}. \tag{5}$$

Ladd *et al.*[30] suggested this time constant corresponds to the mode's relaxation time. Henry and Chen[29] subsequently used this approach to study phonon relaxation times in silicon. This modal analysis technique can provide temperature-, strain, and defect dependent phonon-phonon relaxation times without fitting parameters, which can be used as input to the Boltzmann equation under the relaxation-time approximation.

The Green-Kubo expression for thermal conductivity and modal decomposition methodology separately provide important information about phonon transport in crystalline materials. Combining the two formalisms, however, can elucidate even more information, particularly for systems such as polymer chains, where anomalous heat conduction may be possible.

We begin by expressing the temporally varying heat flux, in terms of the temporally varying phonon occupation numbers.[25] For a one-dimensional (1D) system such as a polyethylene chain we express the heat flux as

$$Q_z = \frac{1}{V}\sum_k \sum_p h\nu v_z \delta n(t), \tag{6}$$

where $h$ is Plank's constant, $v_z$ is the phonon group velocity, and $\delta n$ is the deviation from the average occupation. Inserting Eq. (6) into Eq. (1) results in an expression for thermal conductivity in terms of the normal-mode-mode correlation functions,

$$\kappa = \frac{1}{Vk_BT^2}\sum_k \sum_p \sum_{k'} \sum_{p'} (h\nu h\nu')(vv') \times \int_0^\infty \langle \delta n(t)\delta n'(t+t')\rangle dt'. \tag{7}$$

Here we can make use of Wick's factorization scheme,[25]

$$\langle abcd\rangle = \langle ab\rangle\langle cd\rangle + \langle ac\rangle\langle bd\rangle + \langle ad\rangle\langle bc\rangle, \tag{8}$$

to determine the squared deviation from average $\langle \delta n^2\rangle$, by substituting the creation and annihilation operators $a$ and $a^\dagger$ for the occupation $n$,

$$\begin{aligned}\langle \delta n^2\rangle = \langle n^2\rangle - \bar{n}^2 &= \langle a^\dagger a a^\dagger a\rangle - \bar{n}^2 \\ &= \langle a^\dagger a\rangle\langle a^\dagger a\rangle + \langle a^\dagger a^\dagger\rangle\langle aa\rangle + \langle a^\dagger a\rangle\langle aa^\dagger\rangle - \bar{n}^2 \\ &= \bar{n}(\bar{n}+1),\end{aligned} \tag{9}$$

$$\bar{n} = \left[\exp\left(\frac{h\nu}{k_BT}\right) - 1\right]^{-1}. \tag{10}$$

This then allows us to express the thermal conductivity in terms of the normalized mode correlation functions $\frac{\langle \delta n(t)\delta n'(t+t')\rangle}{\sqrt{\langle \delta n^2(t)\rangle\langle \delta n'^2(t)\rangle}}$ as

$$\kappa = \frac{1}{V}\sum_k \sum_p \sum_{k'} \sum_{p'} k_B \left(\frac{xe^{x/2}}{(e^x-1)}\frac{x'e^{x'/2}}{(e^{x'}-1)}\right)(vv') \times \int_0^\infty \frac{\langle \delta n(t)\delta n'(t+t')\rangle}{\sqrt{\langle \delta n^2(t)\rangle\langle \delta n'^2(t)\rangle}}dt', \tag{11}$$

where $x=h\nu/k_BT$ and the normal-mode correlation function $\frac{\langle \delta n(t)\delta n'(t+t')\rangle}{\sqrt{\langle \delta n^2(t)\rangle\langle \delta n'^2(t)\rangle}}$ can be calculated from the molecular dynamics trajectory data by recognizing that the normalized correlation function for the mode's occupation is equivalent to the normalized correlation function for the mode's energy $\frac{\langle \delta n(t)\delta n'(t+t')\rangle}{\sqrt{\langle \delta n^2(t)\rangle\langle \delta n'^2(t)\rangle}} = \frac{\langle \delta E(t)\delta E'(t+t')\rangle}{\sqrt{\langle \delta E'^2(t)\rangle\langle \delta E'^2(t)\rangle}}$. By identifying the specific heat $C=k_Bx^2\exp(x)[\exp(x)-1]^{-2}$, Eq. (11) can be cast more intuitively as

$$\kappa = \frac{1}{V}\sum_k \sum_p \sum_{k'} \sum_{p'} \sqrt{CC'}(vv') \int_0^\infty \frac{\langle \delta n(t)\delta n'(t+t')\rangle}{\sqrt{\langle \delta n^2(t)\rangle\langle \delta n'^2(t)\rangle}}dt'. \tag{12}$$

Inspection of Eq. (12) reveals several interesting features that bear resemblance to the way thermal conductivity is expressed when derived from the Boltzmann transport equation, using the relaxation-time approximation,[22]

$$\kappa = \frac{1}{V}\sum_k \sum_p Cv^2\tau. \tag{13}$$

Here, the single mode relaxation time $\tau$ still includes all possible phonon-phonon scattering interactions. The key difference between Eqs. (12) and (13) is that the relaxation time in Eq. (13) is based on the Boltzmann equation and assumes that phonon-phonon scattering events are not correlated. The cross terms in Eq. (12), where $k\neq k'$ or $p\neq p'$, account for the possibility that phonon-phonon scattering events could be correlated, which would violate the Stosszahlansatz assumption of molecular chaos.[24] In previous works,[29–31] where molecular dynamics simulations were used to study thermal conductivity, only the terms where $k=k'$ and $p=p'$ were included in accordance with Eqs. (5) and (13). The added correlation features captured by Eq. (12), however, are important for understanding anomalous heat conduction in 1D polyethylene chain molecules. Next we offer an interpretation of Eq. (12) that will lead to a more intuitive explanation for anomalous heat conduction.

## III. SCATTERING AND CORRELATION PARADIGMS

The traditional viewpoint for understanding lattice thermal conductivity is based evaluation of phonon-scattering rates.[22,25] In this paradigm, we begin from the idealization of a perfectly harmonic crystal, where the system's normal modes/phonons are noninteracting. In this limit, the thermal conductivity of the crystal is infinite. The next step is then to consider anharmonicity, which is the degree of departure from this idealization. Anharmonicity leads to umklapp scattering, finite scattering rates, and finite thermal conductivity.[23] From this view point, it is thought that the sequence of scattering events is random,[24,25] and this perspective leads to full consistency with Fourier's law for heat conduction.[22,25] The results of the famous FPU problem, however, are difficult to understand from this view point. From this scattering based paradigm, the FPU system exhibits its phonon-phonon scattering through its mode-mode interactions and should therefore have finite thermal conductivity. It is here that we offer an interpretation of Eq. (12) based on mode-mode correlation rather than scattering, which provides a different way of thinking about anomalous heat conduction.

Consider the opposing limit of a crystal with completely random atomic motion. Although this situation does not occur in nature, it serves as an idealization from which we can deviate in order to investigate the effects of correlation. In this limit, we consider that the motion of every atom as completely independent of the surrounding atoms, such that there

are no atomic interactions to allow two atoms to influence each other's trajectory. We also consider that each atom is localized to a specific region through an onsite potential. This denies each atom the ability to transfer heat by convective diffusion. Although this situation does not occur in nature we have chosen this idealization so that no aspect of the atomic motion is correlated, and therefore if the heat flux autocorrelation function in Eq. (1) were evaluated, the resultant thermal conductivity would be zero. In this idealized limit of random uncorrelated atomic motion, the atoms are noninteracting while in the opposing limit of an idealized perfectly harmonic crystal, the phonons are noninteracting. By proposing this counteridealization to the perfectly harmonic crystal, we can now consider all real materials as a deviation from the uncorrelated limit, as there is always some finite correlation in the atomic motion.

Starting from the limit of uncorrelated motion leads to a correlation based paradigm for thinking about thermal conduction, where the correlation in Eq. (1) now acts as a measure of departure from this limit. From this point of view we consider any form of patterned or correlated motion in the system's trajectory as a contribution to thermal conductivity. For systems where phonons are present, this perspective intuitively accounts for the possibility that scattering events can occur in an ordered sequence. It is important to note here that Eq. (1) measures the amount of correlation in the atomic motion, which is valid for any phase of matter. Equation (12) was derived for a special case, where the system energy is comprised of normal modes and Eq. (6) is valid. As a result, Eq. (12) shows that thermal conductivity is increased by normal-mode correlations in crystalline materials, which derive from the underlying correlation in the atomic motion. To expand on this point, let us postulate the meaning of the temporal fluctuations in mode energy used to calculate the correlations in Eq. (12).

Let us reconsider the classical picture of the idealized perfectly harmonic crystal where the system is initialized with all the energy in one particular mode. This system will perpetually stay in the initial state unless otherwise perturbed. We would therefore observe that the singly excited mode's total energy is constant. If we then add anharmonicity to the particle interactions, however, we would expect the mode's total energy to change with time due to interactions with other modes. We therefore interpret the mode energy fluctuations as a direct measure of the mode-mode interactions (phonon-phonon scattering events) taking place at a given instant.

For three-dimensional (3D) bulk materials where many different scattering events are possible, we would expect the order or sequence of scattering events involving one mode $[k,p]$ to be independent and unrelated to the sequence of scattering events for another mode $[k',p']$. This would be consistent with notion that phonon-phonon collisions are chaotic, which would imply that the cross terms ($k \neq k'$ or $p \neq p'$) of Eq. (12) could be neglected.[24] This simplification would reduce Eq. (12) to Eq. (13). The validity of the molecular chaos assumption is partially supported by the agreement with experiments that was obtained in previous studies that employed Eqs. (5) and (13) for bulk materials.[29,31] For 3D materials we would expect that the number of allowable phonon-phonon scattering events is large and therefore chaotic because many choices for interactions exist. This would imply that the cross terms in Eq. (13) are negligible. For 1D chain lattices, however, the number of allowable scattering events is significantly reduced from that of a 3D bulk material and therefore the assumption of chaotic collisions becomes questionable. From our interpretation, the cross terms of Eq. (12) account for the possibility that the sequence of phonon-phonon scattering events can be temporally correlated, which would lead to an additional contribution to heat conduction.

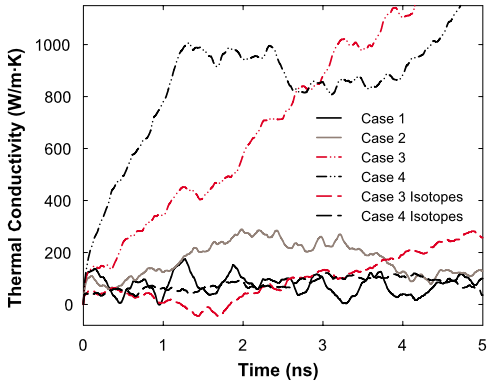


FIG. 1. (Color online) Green-Kubo thermal-conductivity integrals. The results of five independent simulations are shown, which exhibited contrasting behavior. Cases 1–4 use identical simulation parameters and procedures but were initialized with different random velocities. Case 5 uses the same initial velocities as case 4; however the masses of three carbon atoms and five hydrogen atoms were increased to heavier isotopes.

The idea here is that scattering events need not occur randomly, as is generally assumed in the study of heat conduction.[24,25] Any form of correlation or patterning of the atomic motion can add to a material's thermal conductivity. If a system of phonons were to have sequenced or cyclically occurring phonon-phonon scattering events, it could result in mode-mode cross correlation, as indicated by Eq. (12). This therefore suggests that anomalous heat conduction can occur in a system with finite (nonzero) scattering rates. If there is some underlying persistent cyclic or sequenced scattering behavior, this phenomenon could then cause cross correlations in Eq. (12) to remain correlated indefinitely, leading to infinite thermal conductivity.

## IV. SIMULATION PROCEDURES

We used the AIREBO potential[19] to model individual polyethylene chains in the zigzag conformation. The AIREBO potential was implemented in LAMMPS, a parallel molecular dynamics package developed at Sandia National Laboratories.[37] Based on previous results,[15] which showed divergent behavior, we focused on single chains that were 40 unit cells (ucs) in length, where the unit-cell length was $\sim$2.56 Å and the cross-sectional area was taken to be 18 Å$^2$. All simulations used periodic boundary conditions along the length of the chain and were run for 10 ns with a 0.25 fs time step for good energy conservation. Each simu-

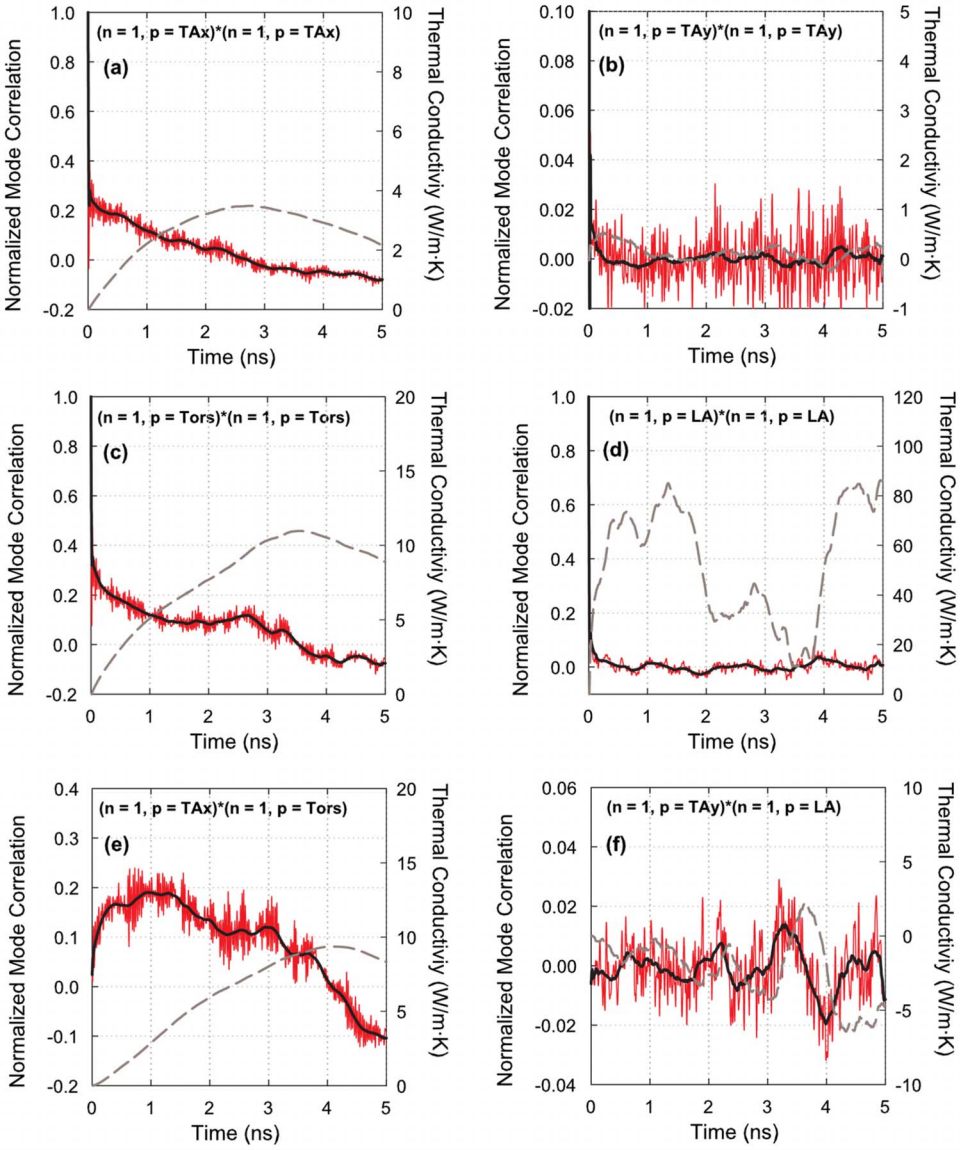


FIG. 2. (Color online) Normal mode correlation functions (fluctuating lines) and thermal-conductivity contributions (gray-dashed lines) for the longest wavelength modes ($\lambda=40$ ucs) of the four acoustic polarizations in case 3. In each panel the correlation corresponds to the two modes indicated by wave-vector index $n$ and polarization $p$. The raw data (left-vertical axis) is shown with light solid thin lines. Smoothed local average values (left-vertical axis) are shown with dark solid thick lines. (a)–(d) show mode autocorrelations while (e) and (f) show cross correlations. In each panel the cumulative contribution to thermal conductivity (right-vertical axis), based on Eq. (12), is shown with gray-dashed lines.

lation was initialized with all atoms in their equilibrium positions, and random velocities corresponding to a quantum corrected room temperature (300 K).[15,34,38]

## V. RESULTS AND DISCUSSION

Of the 60 independent simulations that were run, all of the results discussed in this report correspond to the data obtained from the five example cases shown in Fig. 1, which showed strongly contrasting behavior. As compared to the five cases shown in Fig. 1, all of the other 55 simulations exhibited similar converging/diverging or intermediate behaviors. Cases 1–4 are identical simulations except that the random initial velocities (random number seed) differed, which lead to different phase-space trajectories. Case 5 used the same initial velocities as case 4 but the masses of three randomly selected carbon atoms and five randomly selected hydrogen atoms were changed to heavier isotopes. Figure 1 shows the cumulative integral in Eq. (1) versus the amount of integration time. The large oscillations are due to the fact that each curve corresponds to the results of an individual simulation trajectory. These oscillations are usually suppressed by averaging over many independent simulations. However, for the present investigation we focus on analysis and explanation of the strong divergence in specific simulations.

In Fig. 1, cases 1 and 2 show convergent behavior $\sim$150 W/mK. This type of convergence is similar to what is typically observed for 3D bulk materials.[15,28,31–34,38,39] The heat flux autocorrelation (HFAC) integrals of cases 3 and 4, however, indicate divergence as the HFAC integral continues increasing beyond 1000 W/mK at 5 ns. For most materials, HFAC functions decay within 500 ps.[15,28,31–34,38,39] Here we have extended the integration by an order of magnitude to investigate the long-time behavior for more insight into the infinite time behavior. For cases 3 and 4, the HFAC does not completely decay and has a persistent tail that causes the integral to diverge (Fig. 1). When these same divergent simulations are run with isotopes present, the previously persistent HFAC tails no longer endure, leading to a convergent integral. This response to a physical modification of the

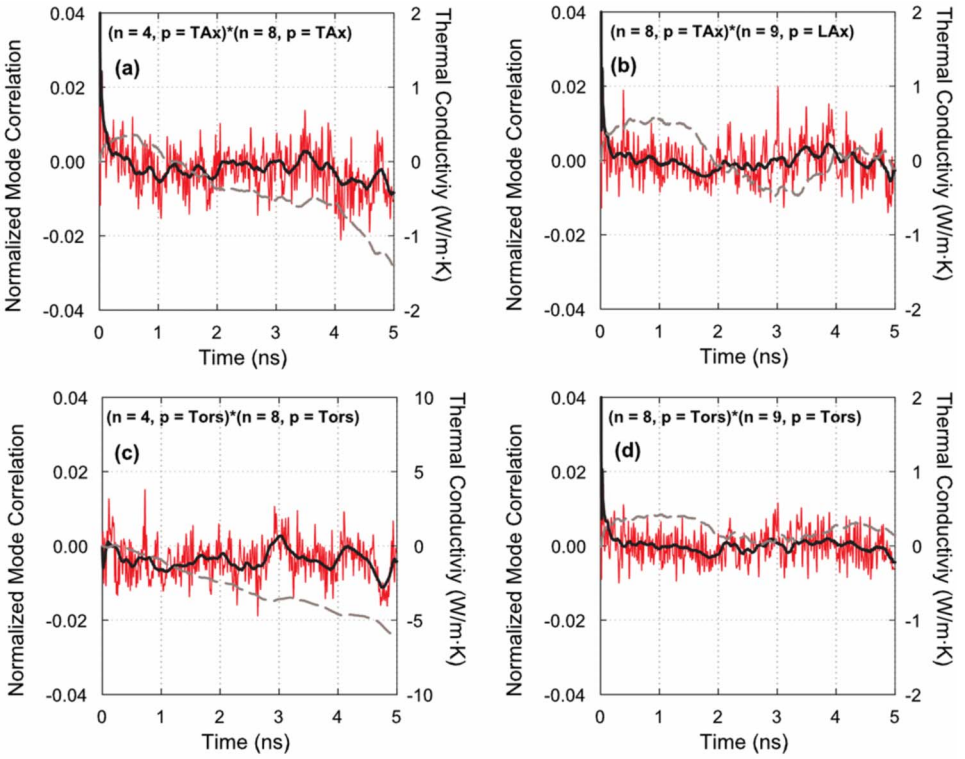


FIG. 3. (Color online) Normal mode cross-correlational functions (fluctuating lines) and thermal-conductivity contributions (gray-dashed lines) for TA$x$ and Tors polarizations in case 3. In each panel the correlation corresponds to the two modes given by wave-vector index $n$ and polarization $p$. The raw data (left-vertical axis) is shown with light solid thin lines. Smoothed local average values (left-vertical axis) are shown with dark solid thick lines. The cumulative contribution to thermal conductivity (right-vertical axis), based on Eq. (12), is shown with gray-dashed lines.

problem suggests that the divergent phenomenon is not a result of unphysical numerical artifacts. Other simulations[15] of longer chains, which also exhibit the same diverging behavior, lend additional support to this notion and suggest that the divergent behavior is a result of a physically meaningful aspect of the nonlinear AIREBO model.

With these five cases under consideration, we used the previously discussed modal analysis technique in conjunction with the Green-Kubo method to calculate the normal-mode correlation functions and their respective contributions to the net thermal conductivity [Eq. (12)]. Figure 2 shows several normal-mode correlation functions corresponding to modes with wavelengths of 40 ucs, for the divergent case 3. In the remaining Figs. 2–6, the value $n$ denotes the wave vector as $k=n2\pi/40$ ucs, while the value for $p$ denotes the corresponding polarization. For the polarizations $p$, we have used the following abbreviations: TA$x$ corresponds to the transverse-acoustic modes with vibrations perpendicular to the C-C bonding plane, TA$y$ corresponds to the transverse-acoustic modes with vibrations in plane with the C-C bonds, LA corresponds to the longitudinal-acoustic modes with vibrations along the chain axis, and Tors corresponds to the torsional acoustic modes, which twist about the chain axis in/out of the C-C bonding plane. Each figure panel contains a title with the two modes and polarizations listed in parentheses. Figures 2(a)–2(d) show the autocorrelation functions for the longest wavelength modes in each acoustic branch (divergent case 3). Other autocorrelation functions for the optical modes were also calculated but they all exhibited decaying behavior with time constants between 0.1–5 ps. Although optical modes have much smaller and often negligible contributions to thermal conductivity, they can play an important role in heat conduction by scattering with acoustic modes.[21]

Decaying behavior was also observed for the acoustic modes; however, Figs. 2(a) and 2(c) show that the TA$x$ and Tors modes behave differently, and do not fully decay within 5 ns. This persistent correlation suggests that these modes do not fully attenuate, which is related to mode-coupling theory based explanations of anomalous heat conduction.[5] Figures 2(b) and 2(d), on the other hand, show that the TA$y$ and LA modes decay within 500 ps, which is consistent with normal diffusive transport even though the decay time is long. The two polarizations that exhibit nonattenuating behavior (TA$x$ and Tors) are the modes that correspond to the out of C-C bonding plane vibrations.

Motivated by mode-coupling theory based explanations of divergent thermal conductivity,[5] the persistent Ta$x$ and Tors correlations were initially thought to be the source of the divergent phenomenon.[15] This idea, however, was unable to explain the divergence alone because the TA$x$ and Tors autocorrelation functions persisted in all cases. Even in cases 1 and 2 where the results converged, these TA$x$ and Tors modes exhibited nonattenuating behavior similar to that of case 3, shown in Figs. 2(a) and 2(c). The idea that this could explain the divergence in Fig. 1 was further invalidated by calculation of each correlation's respective contribution to the thermal conductivity using Eq. (12), which is shown in each panel with the right-side vertical axis. Examination of the cumulative thermal-conductivity contribution for each of these modes, via the integral in Eq. (12), shows that despite the fact that these modes do not fully decay, their contribution to thermal conductivity is only of order 10 W/mK. Contributions of this magnitude are not large enough to account for the rate of divergence observed for cases 3 and 4 in Fig. 1. The LA mode autocorrelation [Fig. 2(d)], however, has a much larger contribution because the LA velocities are

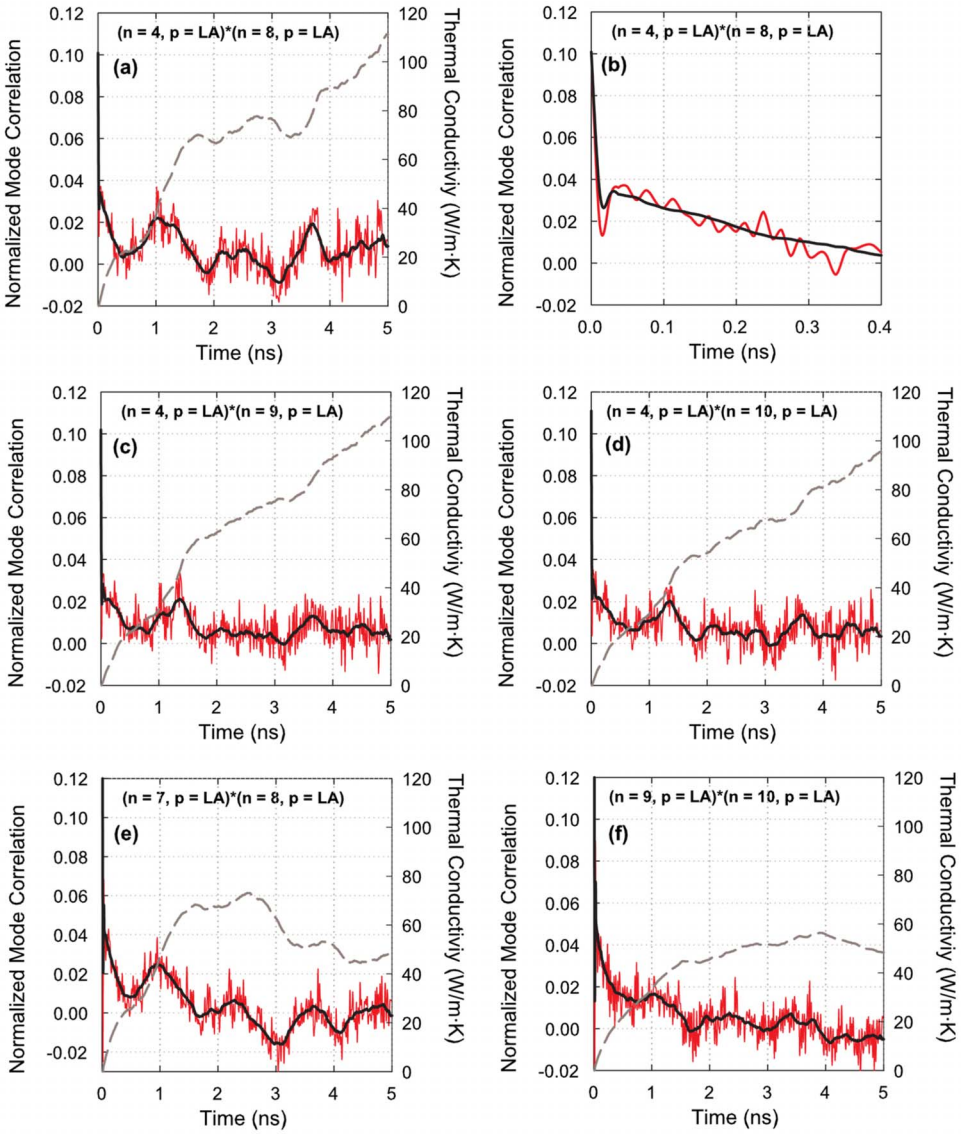


FIG. 4. (Color online) Normal mode correlation functions (fluctuating lines) and thermal-conductivity contributions (gray-dashed lines) for LA modes in case 3. In each panel the correlation corresponds to the two modes indicated by wave-vector index $n$ and polarization $p$. The raw data (left-vertical axis) is shown with light solid thin lines. Smoothed local average values (left-vertical axis) are shown with dark solid thick lines. The cumulative contribution to thermal conductivity (right-vertical axis), based on Eq. (12), is shown with gray-dashed lines. (b) illustrates the short-time behavior of the correlation in (a).

$\sim$16 000 m/s. Although this mode's contribution is stronger, its autocorrelation decays within 500 ps, which cannot account for the positive slope at 5 ns, for case 3 in Fig. 1.

It is interesting to note that, when the normalized mode correlation is negative [Fig. 2(e)], it implies that the fluctuations in mode energy are of opposite sign, such that one mode is above its average energy while the other is below its average energy. For example, if the correlation is negative at time separation $t'$, it means that, on average when the energy in mode $k,p$ is above its average value at $t=t_0$, the energy fluctuations are correlated with those in mode $k',p'$ at time $t=t_0+t'$ while mode $k',p'$ is below its average energy. For mode pairs that share the same sign for their group velocity, this negative correlation can detract from the system's ability to conduct heat. This implies that mode correlations can couple some of the energy from forward-scattering events to backward-scattering events, such that the net effect is to transport heat against the temperature gradient. Although these negative correlation effects can lead to temporarily negative values for thermal conductivity, which can be viewed as a temporary microscopic violation of the second law, the time average behavior is always positive and no negative divergence was observed in any simulation.

By examining Eq. (12) we see that cross correlations can also contribute to the thermal conductivity. Figures 2(e) and 2(f) show cross correlations between the two nonattenuating TA$x$ and Tors modes, as well as the decaying TA$y$ and LA modes which have higher velocities. Even though the cross correlation between the TA$x$ and Tors modes reaches as high as 0.2, implying that 20% of the energy fluctuations are correlated, the corresponding thermal-conductivity contributions are still unable to account for the large persistent slopes in Fig. 1. The panels of Fig. 3 show several cross correlations for shorter wavelength modes in the TA$x$ and Tors polarizations but these cross correlations also show minimal contributions to the thermal conductivity. Although these cross correlations do not explain the divergent results in Fig. 1, the small cross-correlational oscillations in Figs. 2(e), 2(f), and 3(a)–3(d) support the notion that the cross terms of Eq. (12) may be negligible in many cases, particularly for 3D materials where divergent conductivity is not expected.[29,31]

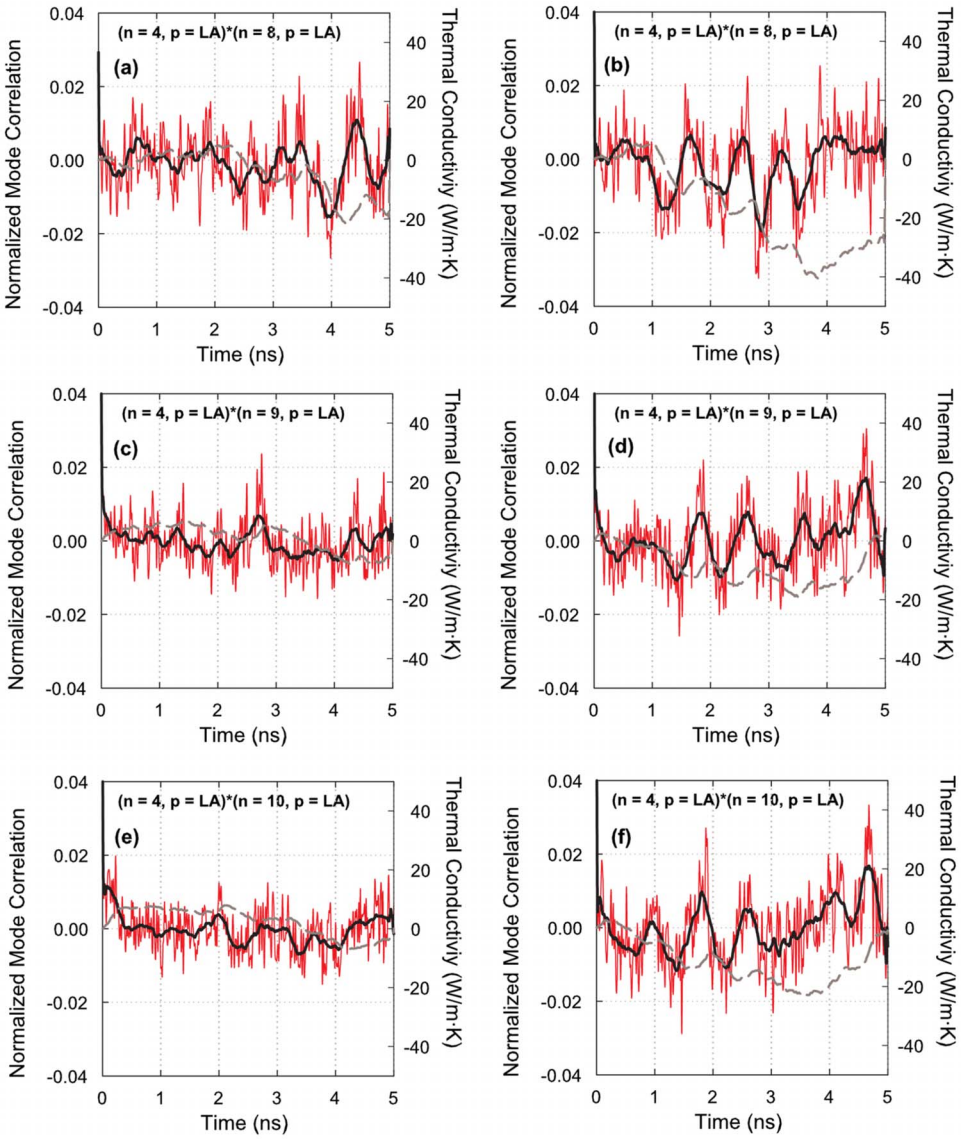


FIG. 5. (Color online) Normal mode correlation functions (fluctuating lines) and thermal-conductivity contributions (gray-dashed lines) for LA modes in cases 1 and 2. (a), (c), and (e) correspond to case 1 while (b), (d), and (f) correspond to case 2. In each panel the correlation corresponds to the two modes indicated by wave-vector index $n$ and polarization $p$. The raw data (left-vertical axis) is shown with light solid thin lines. Smoothed local average values (left-vertical axis) are shown with dark solid thick lines. The cumulative contribution to thermal conductivity (right-vertical axis), based on Eq. (12), is shown with gray-dashed lines.

In order to explain the large rate of divergence in Fig. 1, we can see from inspection of Eq. (12) that the phonon group velocity plays the strongest role in determining contributions to thermal conductivity. A rough inspection of the phonon dispersion for polyethylene[15,35] indicates that correlations between the LA phonons will have the strongest contribution to thermal conductivity. Figure 4 shows several LA cross correlations for the divergent case 3. Figure 4(a) shows that the correlation between the $n=4$ and $n=8$ modes persists up to 5 ns. The corresponding contribution to thermal conductivity is on the order of 100 W/mK, which is five to ten times higher than that of other polarizations. Figure 4(b) shows a very interesting feature of the divergent LA cross correlations at short times. In the first 400 ps, the cross correlation decays with oscillations, bearing strong resemblance to normal-mode autocorrelations. The key feature in Fig. 4(a) is that the cross correlation oscillates with a small positive offset, which causes its integral to increase over the entire duration considered. Several other persistent LA cross correlations are also shown in Figs. 4(c) and 4(d), which indicate that the $n=4$ and $n=8$ cross correlation is not the only combination that gives rise to this diverging trend. Figures 4(e) and 4(f), however, show that not all combinations of LA modes give rise to a persistent tail. Nonetheless, the combined effects of the several different LA mode combinations that have persistent tails, when $\pm k$ values are considered, results in a large enough contribution that can account for the magnitude of the divergent slopes in Fig. 1. A more complete correspondence would require computation of all possible cross-correlational combinations, which is beyond our current computing capability. The results in Fig. 4, however, offer a possible explanation for the divergence observed in the Green-Kubo results of Fig. 1.

To test the results of Fig. 4 as a possible explanation for the divergent HFAC integrals in cases 3 and 4, we also computed LA cross correlations for the convergent cases 1 and 2, which are shown in Fig. 5. Figure 5 shows that when the same cross correlations, which were divergent for case 3 [Figs. 4(a)–4(d)], are computed for the convergent cases 1 and 2, the contributions to thermal conductivity oscillate about zero. This lends support to our explanation for the divergence, which is only associated with cases 3 and 4. This

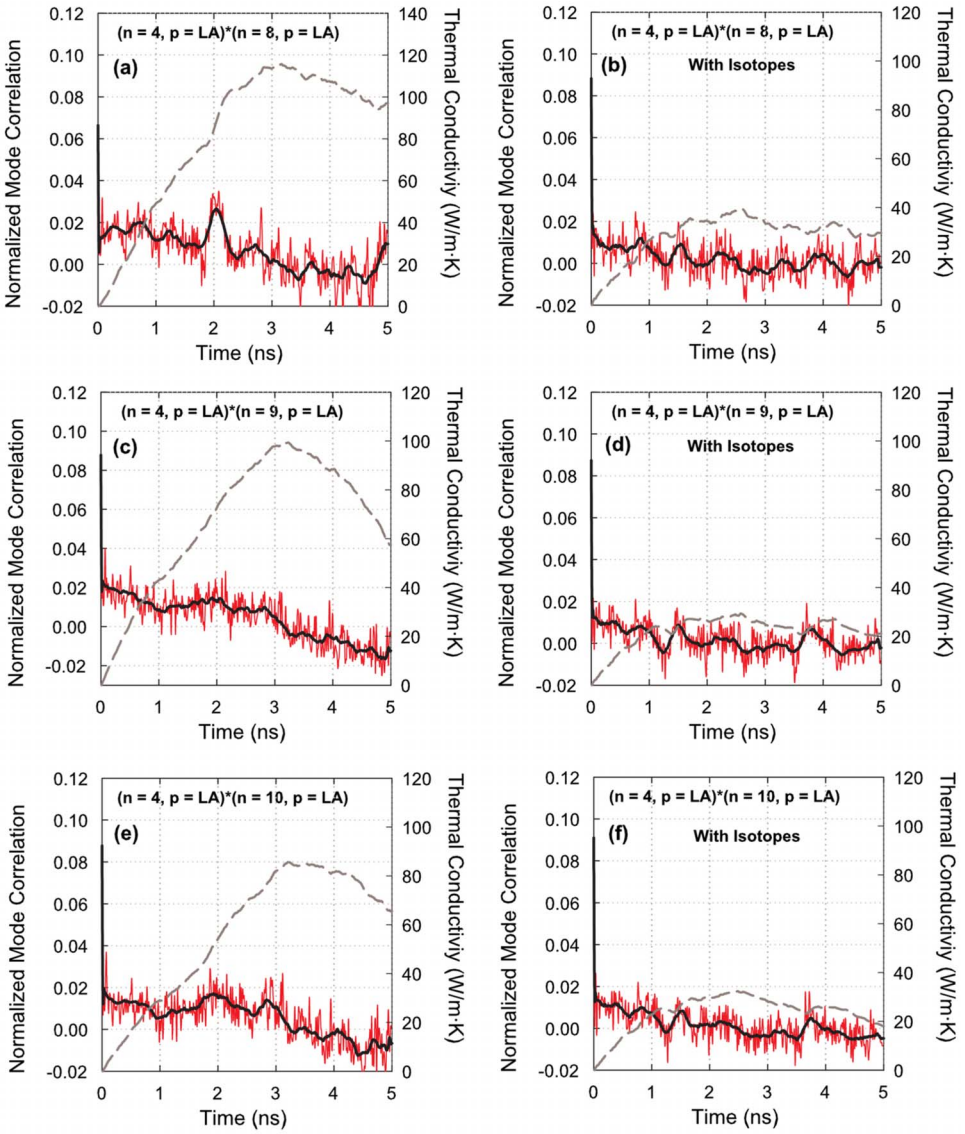


FIG. 6. (Color online) Normal mode correlation functions (fluctuating lines) and thermal-conductivity contributions (gray-dashed lines) for LA modes in cases 4 and 5. (a), (c), and (e) correspond to data from divergent case 4 while (b), (d), and (f) correspond to case 5, which is equivalent to case 4 with the addition of isotopes. In each panel the correlation corresponds to the two modes indicated by wave-vector index $n$ and polarization $p$. The raw data (left-vertical axis) is shown with light solid thin lines. Smoothed local average values (left-vertical axis) are shown with dark solid thick lines. The cumulative contribution to thermal conductivity (right-vertical axis), based on Eq. (12), is shown with gray-dashed lines.

also supports our hypothesis that cross correlations may be negligible in many cases where normal chaotic phonon collisions are expected.

To further test our hypothesis, we also computed LA cross correlations for case 4 and compared them to case 5, which uses the same initial velocities but also includes isotopes. By comparing the correlations and thermal-conductivity contributions in Figs. 6(a), 6(c), and 6(e) with that of Figs. 6(b), 6(d), and 6(f), we see that the presence of isotopes significantly decreases the contribution to thermal conductivity. From the cross-correlational results in Fig. 6, we see that the presence of isotopes inhibits the persistent correlation, which subsequently caused the HFAC divergence for case 4 in Fig. 1.

Based on the results of Figs. 2–6, we believe the HFAC divergence is caused by persistent cross correlations between certain LA modes. This persistent correlation has direct correspondence with our interpretation of Eq. (12) as it relates to our more intuitive explanation of anomalous heat conduction. Although our results only show divergence when the chain length is longer than 40 ucs, Fig. 2(d) does not indicate that the lowest mode in the LA polarization is directly causing the divergence through its own autocorrelation. Its presence in the system may however be necessary for correlations to persist among other LA mode scattering processes. Mode-coupling theories suggest that low-frequency long-wavelength modes behave differently than higher frequency modes, and diffuse slowly over a longer time scale.[5] We do see some consistency with this interpretation through the nonattenuating TA$x$ and Tors modes in Figs. 2(a) and 2(c), respectively. Based on Eq. (12), however, these modes are unable to account for the strong divergence observed in Fig. 1. The persistent cross correlations in Fig. 4 indicate that the midfrequency LA modes may have a cyclically correlated sequence of scattering events. The fact that the autocorrelations for these modes (not shown) decay with convergent contributions to thermal conductivity suggests that these modes have finite nonzero scattering rates. The persistent cross correlations, however, indicate that the scattering events themselves are correlated and do not occur randomly, as is commonly thought. Our evidence and explanation differs from that of previous authors[5] and we believe it deserves

consideration as a possible mechanism for explaining anomalous heat conduction in low dimensional lattices.

## VI. CONCLUSION

We have presented an alternative framework and interpretation of for phonon heat conduction, which allows for an intuitive understanding of anomalous heat conduction in one-dimensional lattices. The proposed interpretation is based on an expression for thermal conductivity which combines the Green-Kubo method with modal analysis. This expression uses phonon creation and annihilation operators to write the thermal conductivity as a summation of normalized autocorrelation and cross-correlational functions. The contributions from autocorrelations have been considered previously in order to extract phonon relaxation times.[15,29–31,33] Our results, however, show that cross correlations between different modes can also have significant contributions, particularly in one-dimensional systems, where anomalous heat conduction is anticipated. The results also indicate that these cross-term contributions may be negligible for most 3D systems, where many possible scattering events exist. For our model of a single polyethylene chain, however, we observe persistent cross correlations between several combinations of midfrequency longitudinal-acoustic modes. These persistent correlations only arise for the simulations that exhibit divergent thermal conductivity and are also able to account for the rate of divergence. As a result we believe the divergent phenomenon exhibited by our model is the result of correlated scattering events among these longitudinal-acoustic modes. Our explanation for anomalous heat conduction in one-dimensional lattices essentially states that the assumption of molecular chaos[24,25] in the Boltzmann equation is invalid for low dimensional systems, where a low number of scattering events are possible. Our correlated scattering event explanation differs from that of previous works,[5] which attribute anomalous heat conduction to the slowly diffusing nonattenuating nature of certain low-frequency modes, based on mode-coupling theory. Although we observed evidence in support of this explanation, evaluation of these modes' contributions to thermal conductivity suggested that they are unable to explain the divergence in our simulations.

## ACKNOWLEDGMENTS

We acknowledge computational resources provided by Intel, funding from the DOE to A.H., and funding from NSF Grant No. CBET-0755825.

[1] E. Fermi, J. Pasta, and S. Ulam, Los Alamos Report No. LA1940, 1955 (unpublished).
[2] G. P. Berman and F. M. Izraileva, Chaos **15**, 015104 (2005).
[3] D. K. Campbell, P. Rosenau, and G. M. Zaslavsky, Chaos **15**, 015101 (2005).
[4] S. Lepri, R. Livi, and A. Politi, Phys. Rev. Lett. **78**, 1896 (1997).
[5] S. Lepri, R. Livi, and A. Politi, Europhys. Lett. **43**, 271 (1998).
[6] S. Lepri, R. Livi, and A. Politi, Phys. Rep. **377**, 1 (2003).
[7] B. Li and J. Wang, Phys. Rev. Lett. **91**, 044301 (2003).
[8] B. Li, L. Wang, and B. Hu, Phys. Rev. Lett. **88**, 223901 (2002).
[9] B. Li, H. Zhao, and B. Hu, Phys. Rev. Lett. **86**, 63 (2001).
[10] F. Mokross and H. Buttner, J. Phys. C **16**, 4539 (1983).
[11] O. Narayan and S. Ramaswamy, Phys. Rev. Lett. **89**, 200601 (2002).
[12] A. V. Savin, G. P. Tsironis, and A. V. Zolotaryuk, Phys. Rev. Lett. **88**, 154301 (2002).
[13] J.-S. Wang and B. Li, Phys. Rev. Lett. **92**, 074302 (2004).
[14] J.-S. Wang and B. Li, Phys. Rev. E **70**, 021204 (2004).
[15] A. Henry and G. Chen, Phys. Rev. Lett. **101**, 235502 (2008).
[16] S. Maruyama, Physica B **323**, 193 (2002).
[17] N. Mingo and D. A. Broido, Nano Lett. **5**, 1221 (2005).
[18] J. J. Freeman, G. J. Morgan, and C. A. Cullen, Phys. Rev. B **35**, 7627 (1987).
[19] S. Stuart, A. B. Tutein, and J. A. Harrison, J. Chem. Phys. **112**, 6472 (2000).
[20] A. S. Henry and G. Chen, Nanoscale Microscale Thermophys. Eng. (to be published).
[21] G. P. Srivastava, J. Phys. Chem. Solids **41**, 357 (1980).
[22] G. Chen, *Nanoscale Energy Transport and Conversion: A Parallel Treatment of Electrons, Molecules, Phonons, and Photons* (Oxford University Press, New York, 2005).
[23] R. Peierls, Ann. Phys. **395**, 1055 (1929).
[24] C. Cercignani, *Theory and Application of the Boltzmann Equation* (Elsevier, New York, 1975).
[25] G. P. Srivastava, *Physics of Phonons* (Hilger, New York, 1990).
[26] J. Hansen and I. McDonald, *Theory of Simple Liquids* (Academic, London, 1986).
[27] R. Hardy, Phys. Rev. **132**, 168 (1963).
[28] Jianwei Che, Tahir Çağin, Weiqiao Deng, and William A. Goddard III, J. Chem. Phys. **113**, 6888 (2000).
[29] A. Henry and G. Chen, J. Comput. Theor. Nanosci. **5**, 141 (2008).
[30] A. J. C. Ladd, B. Moran, and W. G. Hoover, Phys. Rev. B **34**, 5058 (1986).
[31] A. J. H. McGaughey and M. Kaviany, Phys. Rev. B **69**, 094303 (2004).
[32] A. J. H. McGaughey and M. Kaviany, Int. J. Heat Mass Transfer **47**, 1783 (2004).
[33] L. Sun and J. Murthy, Appl. Phys. Lett. **89**, 171919 (2006).
[34] S. G. Volz and G. Chen, Phys. Rev. B **61**, 2651 (2000).
[35] Gustavo D. Barrera, Stewart F. Parker, Anibal J. Ramirez-Cuesta, and Philip C. Mitchell, Macromolecules **39**, 2683 (2006).
[36] M. Dove, *Introduction to Lattice Dynamics* (Cambridge University Press, Cambridge, 2005).
[37] S. Plimpton, J. Comput. Phys. **117**, 1 (1995).
[38] J. Lukes and H. Zhong, ASME Trans. J. Heat Transfer **129**, 705 (2007).
[39] J. Che, T. Cagin, and W. A. Goddard, III, Nanotechnology **11**, 65 (2000).